

Constraining the Origin of Magnetar Flares

Bennett Link*

Department of Physics, Montana State University, Bozeman, Montana, 59717, USA

Department of Physics, Monash University, Melbourne, Victoria 3800, Australia

28 February 2024

ABSTRACT

Sudden relaxation of the magnetic field in the core of a magnetar produces mechanical energy primarily in the form of shear waves which propagate to the surface and enter the magnetosphere as relativistic Alfvén waves. Due to a strong impedance mismatch, shear waves excited in the star suffer many reflections before exiting the star. If mechanical energy is deposited in the core and is converted *directly* to radiation upon propagation to the surface, the rise time of the emission is at least seconds to minutes, and probably minutes to hours for a realistic magnetic field geometry, at odds with observed rise times of $\lesssim 10$ ms for both and giant flares. Mechanisms for both small and giant flares that rely on the sudden relaxation of the magnetic field of the core are rendered unviable by the impedance mismatch, requiring the energy that drives these events to be stored in the magnetosphere just before the flare. A corollary to this conclusion is that if the quasi-periodic oscillations (QPOs) seen in giant flares represent stellar oscillations, they must be excited *by the magnetosphere*, not by mechanical energy released inside the star. Excitation of stellar oscillations by relativistic Alfvén waves in the magnetosphere could be quick enough to excite stellar modes well before a giant flare ends, unless the waves are quickly damped.

Key words:

stars: neutron

1 INTRODUCTION

Soft-gamma repeaters (SGRs) are strongly-magnetized neutron stars with magnetic fields of $B = 10^{14} - 10^{15}$ G that produce frequent, short-duration bursts ($\lesssim 1$ s) of $\lesssim 10^{41}$ ergs in hard x-ray and soft gamma-rays, with the peak luminosity in the burst typically being reached in under 10 ms (*e.g.*, Woods & Thompson 2006; Mereghetti 2008). SGRs occasionally produce giant flares that last ~ 100 s; the first giant flare to be detected occurred in SGR 0526-66 on 5 March, 1979 (Barat et al. 1979; Mazets et al. 1979; Cline et al. 1980), releasing $\gtrsim 6 \times 10^{44}$ erg (Evans et al. 1980), and rising to near its peak luminosity in < 2 ms (Mazets et al. 1979; Hurley et al. 1999). The duration of the initial bright peak was 0.1-0.2 s Mazets & Golenetskii (1981). The August 27th 1998 giant flare from SGR 1900+14 liberated $\gtrsim 4 \times 10^{43}$ erg, with a rise time of < 4 ms (Hurley et al. 1999; Feroci et al. 1999). The duration of the initial peak was ~ 1 s (Hurley et al. 1999). On December 27, 2004, SGR 1806-20 produced the largest flare yet recorded, with a total energy yield of $\gtrsim 4 \times 10^{46}$ ergs and a rise time of < 1 ms (Hurley et al. 2005; Palmer 2005; Terasawa et al. 2005). The duration of the initial peak was ~ 0.2 s (Hurley et al. 2005). All of these energy estimates assume isotropic emission.

The giant flares in SGR 1900+14 (hereafter SGR 1900) and SGR 1806-20 (hereafter SGR 1806) showed rotationally phase-dependent, quasi-periodic oscillations (QPOs) with frequencies from 18 Hz to $\simeq 2$ kHz in SGR 1806 (Israel et al. 2005; Watts & Strohmayer 2006; Strohmayer & Watts 2006; Hambaryan et al. 2011), and 28 Hz to 155 Hz in SGR 1900 (Strohmayer & Watts 2005). In these two giant flares, the Fourier power of the burst drops into the noise above ~ 100 Hz, and in the case of SGR 1806, all of the Fourier power above ~ 100 Hz is in the QPOs. Measured spin down parameters imply surface

* E-mail: link@physics.montana.edu

dipole fields of 6×10^{14} G for SGR 0526-66 (Tiengo et al. 2009), 7×10^{14} G for SGR 1900+14 (Mereghetti et al. 2006), and 2×10^{15} G for SGR 1806-20 (Nakagawa et al. 2008). These strong inferred fields, along with other properties such as quiescent brightness (Thompson & Duncan 1995, 1996; Woods & Thompson 2006), establish these objects as magnetars.

Anomalous x-ray pulsars (AXPs) are also magnetars that exhibit bursts that are in most respects like SGR flares, but with a wider range of burst durations. These bursts are generally less energetic than SGR flares, with the most energetic bursts showing much harder spectra than are seen in SGR bursts (see, *e.g.*, Gavril et al. 2004 and Kaspi 2007).

In addition to these high-field objects, there are now three known “low-field” magnetars that produce small flares. SGR 0418+5729 has an inferred dipole field of 6×10^{12} (Rea et al. 2013), typical of radio pulsars. Swift J1822.3-1606 has an inferred dipole field of $\sim 2 \times 10^{13}$ G (Rea et al. 2012; Scholz et al. 2012), while 3XMM J185246.6+003317 has an inferred field of $< 4 \times 10^{13}$ G (Rea et al. 2013). These sources show that magnetar activity does not require high dipolar fields. Instead, the activity could be driven by decay of multipolar components that could be an order of magnitude or more larger than the dipolar component (Braithwaite 2009). These bursts are rather different than SGR bursts. The total energy release is $\lesssim 10^{41}$ erg, like small flares in SGRs, but with decay times of hundreds of days. The timing resolution is insufficient to ascertain how the rise times compare to bursts in SGRs. The long relaxation time is consistent with the thermal relaxation time predicted for the crust (Brown & Cumming 2009; Scholz et al. 2012).

While energetics considerations strongly suggest that SGR flares are driven by the release of magnetic energy (see §2), the trigger mechanism for flares remains unknown. Thompson & Duncan (2001) have argued that the elastic crust cannot store nearly enough elastic energy to power a giant flare, but that the crust can act as a gate that holds back much more magnetic energy. In this connection, Thompson & Duncan (2001) have proposed that the core field evolves into a twisted configuration through Hall drift, stressing the crust until it suddenly yields, producing impulsive energy release throughout the stellar interior. A second possibility is that a magnetohydrodynamic (MHD) instability occurs in the liquid core (Thompson & Duncan 1995). This possibility might appear unlikely, since the core is expected to be superconducting and the proton-electron mixture will have a very high electrical conductivity, but as Flowers & Ruderman (1977) pointed out and Thompson & Duncan (1995) have stressed, if the core field is stabilized by crust currents, and these currents have time to decay, the core field could suffer an interchange instability over MHD time-scales. Moreover, if the core field exceeds $\sim 10^{16}$ G, the core will not be superconducting, the electrical conductivity will be lower, and the field might evolve to the point that an MHD instability occurs. A third possibility is that the energy is released not inside the star, but in the magnetosphere through an MHD instability (Lyutikov 2003, 2006; Komissarov et al. 2007; Gill & Heyl 2010), such as the “tearing mode”, producing a magnetospheric explosion akin to coronal mass ejections seen in the Sun.

Duncan (1998) predicted that magnetic stresses that arise as the internal field of a magnetar evolves will eventually shear the crust to failure, producing a flare and exciting torsional modes in the crust.¹ The QPOs seen in the giant flares of SGRs 1900 and 1806 were interpreted initially as crustal modes (*e.g.*, Piro 2005; Samuelsson & Andersson 2006; Watts & Reddy 2007; Lee 2007; Sotani et al. 2007; Steiner & Watts 2009). Subsequent work has accounted for magnetic coupling between the crust and liquid core, and attributes QPOs to *global* magneto-elastic oscillations of the neutron star (*e.g.*, Levin 2006; Glampedakis et al. 2006; Levin 2007; Sotani et al. 2008; Colaiuda et al. 2009; Cerdá-Durán et al. 2009; Colaiuda & Kokkotas 2011; van Hoven & Levin 2011; Gabler et al. 2011; van Hoven & Levin 2012; Gabler et al. 2012, 2013; Passamonti & Lander 2013a,b). A crucial ingredient in the interpretation of QPOs as stellar oscillations is to understand how crust movement can produce the large observed modulations of the x-ray emission by 10-20%. Timokhin et al. (2008) propose that twisting of the crust, associated with a stellar mode, modulates the charge density in the magnetosphere, creating variations in the optical depth for resonant Compton scattering of the hard x-ray photons that accompany the flare. In this model, the shear amplitude at the stellar surface must be as large as 1% of the stellar radius, and it is unknown if the stellar crust can sustain the associated strain without failing. D’Angelo & Watts (2012) have shown that beaming effects can increase the amplitude of the QPO emission by a factor of typically several. As the theory of neutron star “seismology” is further developed, the exciting possibility of constraining the properties of dense matter and the magnetic field configuration of the core is becoming feasible.

This paper is concerned with the basic question of whether the energy that drives SGR flares is stored in the stellar interior or in the magnetosphere just before the flare occurs. A key physical feature is the existence of a large impedance mismatch between the stellar interior and the magnetosphere for the propagation of shear waves, as originally pointed out by Blaes et al. (1989); the mismatch is due to the fact that the wave propagation speed in the core is $\sim 10^{-3}$ of that in the magnetosphere. With minimal assumptions, I show that shear waves produced in the core through sudden global relaxation of the magnetic field are prevented from quickly entering the magnetosphere by the impedance mismatch; rather, the outer regions of the star and the magnetosphere are highly reflective to shear waves, causing waves to remain trapped in the core for at least seconds to minutes, and perhaps as long as minutes to hours for a realistic magnetic field geometry. The trapping time

¹ In general excitation of many stellar modes, including *p*-modes, *g*-modes, and *f* modes should occur, but torsional modes have the lowest frequencies and would be the easiest to detect.

greatly exceeds typical rise times of < 10 ms, requiring that the energy that powers both small and giant flares is stored in the magnetosphere just before the flare. The energy could then be quickly released through a magnetic instability as proposed by Lyutikov (2003); see, also, Lyutikov (2006) and Komissarov et al. (2007). The energy could be stored in the magnetosphere if, for example, the internal field gradually untwists, slowly twisting the magnetosphere until it becomes unstable (Lyutikov 2003).

Thompson & Duncan (1995) and Thompson & Duncan (2001) have proposed that flares arise from the deposition of magnetic energy *inside* the star. In the model of Thompson & Duncan (2001), both small and giant flares are driven by *sudden* relaxation of a globally-twisted internal magnetic field, with the energy release gated by crust rigidity. When the crust is stressed to failure in this model, the magnetic foot points are suddenly sheared, and energy flows from the stellar interior into the magnetosphere, producing a radiative event through the dissipation of Alfvén waves and magnetic reconnection. Thompson & Duncan (2001) assume that the failure of the crust along the fault allows flow of energy from the core into the magnetosphere over a time-scale of order the Alfvén crossing time of the star or shorter. As shown in this paper, though, the impedance mismatch between the core and the magnetosphere slows the flow of mechanical energy to at least 10^2 to 10^4 Alfvén crossing times (seconds to minutes). Crust failure cannot remove this fundamental mismatch, and so the proposal of Thompson & Duncan (1995) and Thompson & Duncan (2001) that both large and small magnetar flares are driven by the sudden release of magnetic energy stored *inside* the star appears to be unviable.

If flares indeed originate as magnetospheric explosions, energy will be trapped on closed magnetic field lines in the form of relativistic Alfvén waves. The impedance mismatch between the magnetosphere and the stellar interior makes the star highly reflective to these waves. I obtain a lower limit for the time-scale required for relativistic Alfvén waves excited by a magnetospheric explosion to excite magneto-elastic modes in the star, and find that such modes could be excited well before a giant flare ends. Hence, a viable explanation for the QPOs is that they represent stellar oscillations excited *by the magnetosphere*, not the stellar interior, provided the excitation can occur before the waves are damped.

In §2, I discuss general considerations of the release of energy in giant flares. In §3, I formulate the problem of transmission from the deep stellar interior to the surface in a planar geometry, and estimate the transmission coefficient at low frequency. In §4, I calculate the transmission coefficient as a function of frequency, accounting for the material properties of the crust and the strong gradient in the wave propagation speed. In §5, I give numerical results. In §6, I discuss trapping of energy in the core. In §7, I discuss how a realistic magnetic field geometry will greatly decrease the transmission efficiency. In §8, I discuss the trapping of energy in the magnetosphere. An explanation of the similarities and differences between flares in SGRs, low-field magnetars, and AXPs is beyond the scope of this paper, but the basic ideas set forth here apply to all three classes of objects.

2 ENERGY RELEASE IN GIANT FLARES

2.1 Length Scale

Suppose that the magnetic configuration within a volume l^3 inside the star adjusts, lowering the magnetic energy, ultimately driving a flare of radiative energy E . By energy conservation, E is bounded by

$$E < \frac{B^2}{8\pi} l^3, \quad (1)$$

where B is the average field strength. This is an upper limit since the field will not be reduced to zero, and the conversion of magnetic energy to radiation will not be perfectly efficient. The length scale l has a lower limit of

$$l \gtrsim 6 \left(\frac{E}{10^{46} \text{ erg}} \right)^{1/3} B_{15}^{-2/3} \text{ km}, \quad (2)$$

comparable to the stellar radius for a giant flare. Here $B_{15} \equiv B/10^{15}$, and B is measured in Gauss.

2.2 Power Spectrum of the Energy Deposition

Readjustment of the magnetic field configuration occurs through the production of Alfvén waves in the core and magneto-elastic shear waves in the crust; see §3. I will refer to both kinds of waves as “shear waves”, since their properties are the same. Independent of how the magnetic energy is gated or released, the volume l^3 will fill with shear waves over a time-scale $T = l/c_s$, where c_s is the speed of shear waves, typically $3 \times 10^{-3}c$ throughout most of the star; see eqs. [8] and [9] below. The power spectrum of the shear waves that are produced will have a cut-off at $\nu_c \sim 1/T$:

$$\nu_c \equiv \frac{1}{T} = \frac{c_s}{l} \lesssim 200 \text{ Hz } B_{15}^{7/6} \left(\frac{E}{10^{46} \text{ erg}} \right)^{-1/3}, \quad (3)$$

assuming that the protons of the core form a type II superconductor, so that c_s is given by eq. [8]. If the core protons are normal, the estimate remains the same, though the scaling with B changes to $B^{5/3}$. From the energy yields of the three giant flares to date, eq. [3] gives $\nu_c \sim 1.3$ kHz for SGR 1900, 500 Hz for SGR 0526, and 130 Hz for SGR 1806.

In the picture model of Thompson & Duncan (2001) involving relaxation of a twisted internal field, the relevant length scale for the initial deposition of shear waves is the stellar radius, and the high-frequency cut-off will be $\nu_c \sim c_s/R \sim 100$ Hz. This estimate does not depend on whether the magnetic energy is released through a global instability, or if it is gated by crust rigidity.

Based on these estimates, the subsequent analysis will be for the propagation of seismic energy at frequencies below 1 kHz.

3 TRANSMISSION OF ENERGY FROM THE STELLAR INTERIOR TO THE MAGNETOSPHERE

I now calculate the efficiency with which energy deposited in the stellar interior through global readjustment of the field is transmitted to the magnetosphere. For magnetic energy that is released in the stellar interior, the energy will be deposited as heat, sound waves, and shear waves. Thermal energy diffuses through the star relatively slowly - *e.g.*, over a time-scale of months through the crust (Brown & Cumming 2009; Scholz et al. 2012); the energy propagates much more quickly to the surface as mechanical waves. The core supports magnetic shear waves and sound waves. Shear waves propagate along field lines, and the fluid is essentially incompressible (Levin 2006).

The crust supports shear waves, modified by the magnetic field, and sound waves. If a medium that supports shear is driven to failure, most of the wave energy will be in the form of shear waves if the shear wave speed is less than the sound speed (Blaes et al. 1989).² This is the case throughout the core and near the base of the inner crust.

For energy to leave the core, it must propagate along field lines that pass from the core, through the crust, and into the magnetosphere. The plasma density is low in the magnetosphere, so energy propagates there as relativistic Alfvén waves and as magnetosonic waves. Hence, the most efficient way for energy to leave the core is to propagate along field lines that point nearly radially outward. Outgoing shear waves will couple most directly to Alfvén waves in the magnetosphere, and I ignore the weaker coupling to magnetosonic waves. I also note that each reflection of a shear wave in the star will convert some of the energy to compressional waves. I ignore this effect as well, and consider the problem of the propagation of shear waves from the core and crust, and their emission from the star as Alfvén waves.

Consider a simple planar geometry, with the crust-core boundary in the $x - y$ plane at $z = 0$, and the stellar surface at $z = z_s$. The magnetic field is constant and directed along the z axis. A linearly-polarized shear perturbation of displacement $u(z, t) = u(z)e^{-i\omega t}$ obeys (Blaes et al. 1989)

$$\frac{d}{dz} \left(\tilde{\mu} \frac{du}{dz} \right) + \tilde{\rho} \omega^2 u = 0, \quad (4)$$

where

$$\tilde{\mu} \equiv \mu + \frac{B^2}{4\pi}. \quad (5)$$

Here μ is the material shear modulus, which is non-zero only in the crust, and

$$\tilde{\rho} \equiv \rho_d + \frac{B^2}{4\pi c^2}, \quad (6)$$

where ρ_d is the *dynamical* mass density, that is, the mass density associated with matter that moves in response to a passing shear wave. In the inner crust, Bragg scattering of free neutrons with the nuclear lattice gives $\rho_d < \rho$ (Chamel 2005, 2012, 2013; see eq. 19 below). The second term in eq. [6] is the contribution of the magnetic energy to the effective mass of the matter, and is important only near the stellar surface, for $\rho \lesssim 10^8 B_{15}^2 \text{ g cm}^{-3}$. The speed of shear waves is $c_s = \sqrt{\tilde{\mu}/\tilde{\rho}}$. From eq. [4], continuity in u requires that the traction $\tilde{\mu} du/dz$ be everywhere continuous.

The protons of the outer core are expected to form a type-II superconductor (SC) if the field is below the upper critical field $H_{c2} \sim 10^{16}$ G. Type-II superconductivity modifies the magnetic stress. Repeating the derivation of Blaes et al. (1989) using the magnetic stress tensor of Easson & Pethick (1977) gives

$$\tilde{\mu} = \frac{H_{c1} B}{4\pi} \quad (\text{SC core protons}), \quad (7)$$

where $H_{c1} \simeq 10^{15}$ G is the lower critical field. In the core, the protons and neutrons are expected to form distinct superfluids, with negligible nuclear entrainment of the neutron mass current by the proton mass current (Chamel & Haensel 2006; Link

² For material failure through local stresses, the lowest-order emission process of waves is quadrupolar. The energy density in a wave of propagation speed v_p scales as v_p^{-6} .

2012). Here magnetic waves are supported by the charged component, and ρ_d is nearly equal to the proton mass density. If the core is a type II superconductor as predicted, magnetic disturbances propagate as *vortex-cyclotron waves* (Mendell 2002) at speed

$$c_{vc} = \sqrt{\frac{BH_{c1}}{4\pi\rho x_p}} = 3 \times 10^{-3} H_{c1,15}^{1/2} B_{15}^{1/2} \left(\frac{\rho_{14}}{2}\right)^{-1/2} \left(\frac{x_p}{0.05}\right)^{-1/2} c \quad (\text{SC core protons}), \quad (8)$$

where $\rho_{14} \equiv 10^{14} \rho$, ρ is in g cm^{-3} , and x_p is the proton mass fraction. Here fiducial values typical of the outer core have been chosen.

If the core protons are instead normal, waves propagate as Alfvén waves at speed

$$c_A = \frac{B}{\sqrt{4\pi\rho x_p}} = 3 \times 10^{-3} B_{15} \left(\frac{\rho_{14}}{2}\right)^{-1/2} \left(\frac{x_p}{0.05}\right)^{-1/2} c \quad (\text{normal core protons}) \quad (9)$$

In the magnetosphere, $\tilde{\mu} = B^2/4\pi$ and $\tilde{\rho} \simeq B^2/4\pi c^2$, and the Alfvén waves are relativistic:

$$\frac{d^2 u}{dz^2} + \frac{\omega^2}{c^2} u = 0. \quad (10)$$

where the wavenumber in the magnetosphere is $k = \omega/c$.

The wavenumber in the core is $k_c = \omega_s/c_s$, where $c_s = c_{vc}$ for SC core protons and $c_s = c_A$ for normal core protons. For sufficiently low frequencies that $k_c \Delta R \ll 1$ is satisfied, corresponding to $\nu \lesssim 100$ Hz, the wave is insensitive to the gradients in $\tilde{\mu}$ in the crust, and the crust can be treated as a thin discontinuity; crust structure is unimportant in this limit. In this case, the energy transmission coefficient takes the familiar form

$$T = \frac{4(\tilde{\mu}_c k_c)(\tilde{\mu}_m k)}{(\tilde{\mu}_m k + \tilde{\mu}_c k_c)^2}, \quad (11)$$

where $\tilde{\mu}_c = BH_{c1}/4\pi$ for a superconducting core, $B^2/4\pi$ for a core of normal protons and superfluid neutrons, and $\tilde{\mu}_m = B^2/4\pi$ for the magnetosphere. (Recall that B is constant in the assumed planar geometry). Typically $\tilde{\mu}_c k_c \gg \tilde{\mu}_m k$, giving, for a superconducting core,

$$T \simeq 4 \left(\frac{B}{H_{c1}}\right) \frac{c_{vc}}{c} \simeq 10^{-2} \left(\frac{B}{H_{c1}}\right)^{3/2} \left(\frac{x_p}{0.05}\right)^{-1/2} \left(\frac{\rho_{14}}{2}\right)^{-1/2} \quad (\text{SC core protons}). \quad (12)$$

while for a core of normal protons

$$T \simeq 4 \frac{c_A}{c} \simeq 10^{-2} B_{15} \left(\frac{x_p}{0.05}\right)^{-1/2} \left(\frac{\rho_{14}}{2}\right)^{-1/2} \quad (\text{normal core protons}). \quad (13)$$

Because $\tilde{\mu}_c k_c \gg \tilde{\mu}_m k$, there is a strong impedance mismatch between the core and the magnetosphere, giving $T \ll 1$ for $\nu \lesssim 100$ Hz. We will see that T is further reduced by the structure of the crust for $\nu \gtrsim 100$ Hz.

Energy that is released primarily in the core cannot propagate directly to the surface, but becomes trapped in the core. For energy to propagate into the magnetosphere, it must then propagate from the core and through the crust, suffering multiple reflections before escaping to the magnetosphere.

4 ENERGY TRANSMISSION COEFFICIENT

I now turn to an exact calculation of the energy transmission coefficient T for $\nu \gtrsim 100$ Hz, when $k_c \Delta R \ll 1$ is not satisfied, and crust structure has important effects for wave propagation.

The shear modulus in the crust, ignoring magnetic effects, is (Strohmayer et al. 1991)

$$\mu = \frac{0.1194}{1 + 0.595(173/\Gamma)^2} \frac{n_i (Ze)^2}{a}, \quad (14)$$

where n_i is the number density of ions of charge Ze , a is the Wigner-Seitz cell radius given by $n_i 4\pi a^3/3 = 1$, and $\Gamma \equiv (Ze)^2/(akT)$ where k is Boltzmann's constant. Typically in the crust, $\Gamma \gg 173$ and the second term in the denominator is negligible. For the composition of the crust, I use the results of Haensel & Pichon (1994) for the outer crust, and the results of Douchin & Haensel (2001) for the inner crust, conveniently expressed analytically by Haensel & Potekhin (2004), who treat densities from 10^5 g cm^{-3} to above nuclear density. The treatment by Douchin & Haensel (2001) of the inner crust gives somewhat higher values of the shear modulus at the base of the crust than do other studies. The equation of state of Akmal et al. (1998), for example, gives a shear speed at the base of the crust that is about 0.6 the shear speed of Douchin & Haensel (2001), and a corresponding shear modulus that is smaller by a factor of about 2.8. A higher shear speed in the crust decreases the impedance mismatch with respect to magnetosphere, giving somewhat higher values for the transmission coefficient than most other choices of the shear modulus would give.

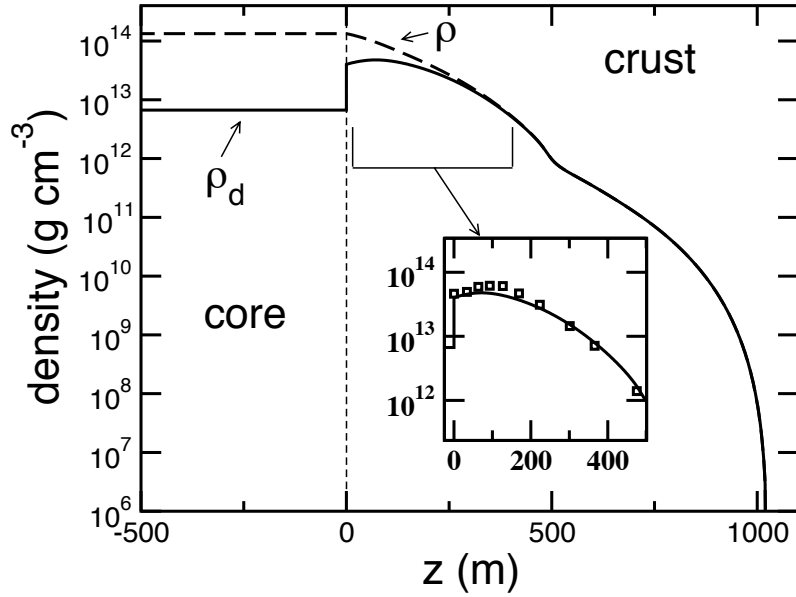


Figure 1. The density profile in the inner crust and outer core. The dashed curve gives the baryonic mass density profile from the solution to eq. [15] with the equation of state of Haensel & Potekhin (2004). The solid curve shows the dynamical mass density of eq. [19]. In the denser regions of the inner crust, $\rho_d < \rho$ from the effects of nuclear entrainment (Chamel 2005, 2012, 2013); see eq. [19]. The inset shows detail of the region where nuclear entrainment effects are most important; the squares are from the calculations of Chamel (2012). In the core, ρ_d is equal to the proton mass density, here fixed to be the density $x_p \rho_c = 6.5 \times 10^{13} \text{ g cm}^{-3}$ at the crust-core interface.

For a barytropic equation of state $p(\rho)$, the density profile in the crust, neglecting the effects of General Relativity, follows from the equation of hydrostatic equilibrium

$$\frac{d\rho}{dr} = -g\rho(r) \left(\frac{dp}{d\rho} \right)^{-1}, \quad (15)$$

where g is the gravitational acceleration. Henceforth I fix $g = 2 \times 10^{14} \text{ cm s}^{-2}$, appropriate to a neutron star of 1.4 solar masses and a radius of 10 km. I take the crust to dissolve into the core at $\rho_c = 1.3 \times 10^{14} \text{ g cm}^{-3}$, about half of nuclear saturation density. Under these assumptions, the crust thickness ΔR is almost exactly 1 km. The density profile in the crust is given by the dashed line in Fig. 1.

I take the core to be of constant density and infinite extent for $z < 0$, with a wave incident on the crust-core interface, and a reflected wave:

$$u(z) = Ae^{ik_c z} + Be^{-ik_c z}, \quad (16)$$

where A and B are constants. Requiring continuity in u and $\tilde{\mu} du/dz$ at the crust-core interface ($z = 0$), gives the transmission coefficient

$$T = 1 - \left| \frac{B}{A} \right|^2 = 1 - \left| \frac{\tilde{\mu}(0-)u(0+)k_c + i\tilde{\mu}(0+)u'(0+)}{\tilde{\mu}(0-)u(0+)k_c - i\tilde{\mu}(0+)u'(0+)} \right|^2, \quad (17)$$

where a prime denotes a derivative in z .

At the surface $z = z_s = \Delta R$, there is only an outgoing relativistic Alfvén wave $e^{ik(z-z_s)}$ with $k = \omega/c$. Since A and B are unspecified, u is conveniently fixed to unity at the surface. Continuity in $\tilde{\mu} du/dz$ gives the surface boundary condition

$$\tilde{\mu}(z - z_s = 0-)u'(z - z_s = 0-) = ik\tilde{\mu}(z - z_s = 0+) \quad \text{with} \quad u(z - z_s = 0-) = 1. \quad (18)$$

The amplitude u becomes complex for $z < z_s$. Calculation of the quantities $u(0+)$ and $u'(0+)$ by numerical integration from the surface to $z = 0$ gives the transmission coefficient from eq. [17].

In the inner crust, most of the baryonic mass is in the form of superfluid neutrons. As a shear wave passes, a fraction of the superfluid neutrons is non-dissipatively entrained by the nuclear clusters through Bragg scattering (Chamel 2005, 2012); the remaining ‘‘conduction’’ neutrons, that is, the neutrons that are not entrained, must be subtracted from the baryonic density to give the appropriate dynamical density (Pethick et al. 2010):

$$\rho_d = \rho(1 - n_n^c/\bar{n}) \equiv f\rho, \quad (19)$$

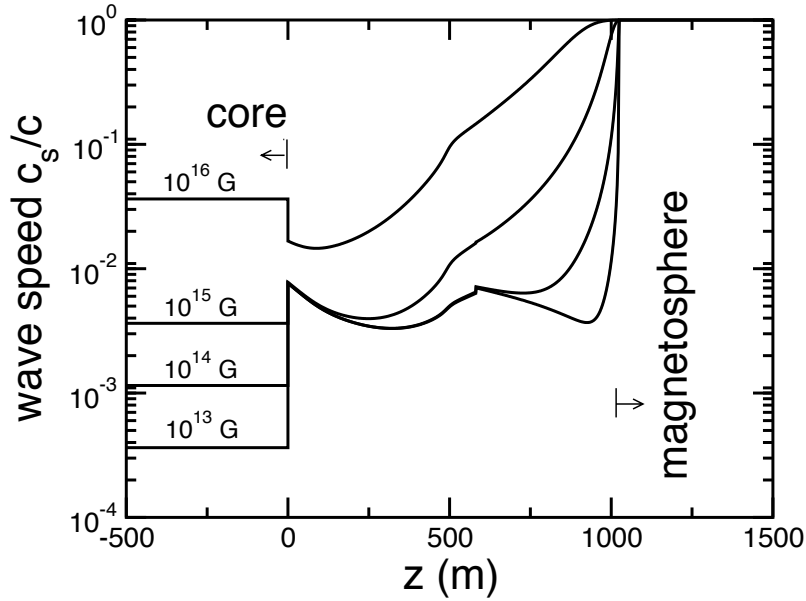


Figure 2. The shear speed $c_s = \sqrt{\tilde{\mu}/\tilde{\rho}}$ as a function of position. As the magnetic field is increased, the effective shear modulus $\tilde{\mu}$ increases in the crust; see eq. [5]. For $B = 10^{16}$ G $\simeq H_{c2}$, the core is taken to be normal. The core neutrons are assumed to be superfluid. Outside the star, the shear speed is c , the speed of a relativistic Alfvén wave. There is a small jump in μ at $z \simeq 600$ m, corresponding to the neutron drip density that is washed out by magnetic stresses for $B \gtrsim 3 \times 10^{14}$ G.

where n_n^c is the number density of conduction neutrons and \bar{n} is the average baryon density in a unit cell. The speed of shear waves in the crust (for $B = 0$) is $c_s = \sqrt{\mu/\rho d}$; the existence of conduction neutrons increases the shear speed. To account for this effect, a fitting formula for f that gives a good approximation to the results of Chamel (2012) is

$$f = 1 - \frac{8.8\bar{n}}{1 + \exp(10^3(\bar{n} - 0.09))} \quad \bar{n} < 0.08 \text{ fm}^{-3}. \quad (20)$$

f stays near unity up to $\bar{n} \simeq 0.04 \text{ fm}^{-3}$, before falling to ~ 0.35 at $\bar{n} = 0.08 \text{ fm}^{-3}$, at which point the inner crust ends. The inset of Fig. 1 shows the assumed dynamical density based on the results of Chamel (2012). The shear speed in the star is shown in Fig. 2.

The inner core could reach a density of $5 - 10\rho_c$, but the gradients in $\tilde{\rho}$ and $\tilde{\mu}$ are always much less than in the inner crust. Some of the energy that is propagating outward will be reflected by the relatively small gradients in $\tilde{\rho}$ and $\tilde{\mu}$ in the core. Treating the core as having constant density slightly overestimates the transmission coefficient. Also, the choice of a constant field in the z direction is the most favourable geometry for the propagation of energy out of the core, through the crust, and into the magnetosphere. Any other field configuration will lead to more effective reflection of energy from the crust and the magnetosphere back into the core. For realistic field configurations, this effect could be large. As argued in §7, these calculations of the transmission coefficient probably represent *significant* overestimates, so the energy transmission efficiency calculated in this paper is a robust upper limit.

5 NUMERICAL RESULTS

Calculations of the transmission coefficient are shown in Fig. 3 for different values of the magnetic field strength, assuming that the core neutrons are superfluid. For each solid curve, the core was assumed to be a type II superconductor. For each dashed curve, the core protons are assumed to be normal - the two curves coincide for $B = H_{c1} = 10^{15}$ G. For $\nu \lesssim 100$ Hz, $k_c \Delta R \ll 1$, and T is nearly independent of frequency. For $B < H_{c1}$, type II superconductivity increases the magnetic stress in the core by a factor $(H_{c1}/B)^{1/2}$ relative to the normal case (see eqs. 12 and 13), giving a corresponding increase in T by decreasing the impedance mismatch between the core and the magnetosphere; see eq. [11]. For $B > H_{c1}$, the situation is reversed, and superconductivity decreases T . A field of $B = 10^{16}$ G is close to the upper critical field H_{c2} above which superconductivity is destroyed; only the dashed curve is likely to be relevant for $B = 10^{16}$ G.

Above $\nu \sim 100$ Hz, gradients in the crust of the density and the shear modulus act as an effective potential which partially reflects the wave back into the core, reducing T . At $\nu \sim 1$ kHz, the solution shows strong transmission resonances that are a consequence of the assumed planar geometry and constant field. More realistic field structure and energy deposition geometry will eliminate these resonances.

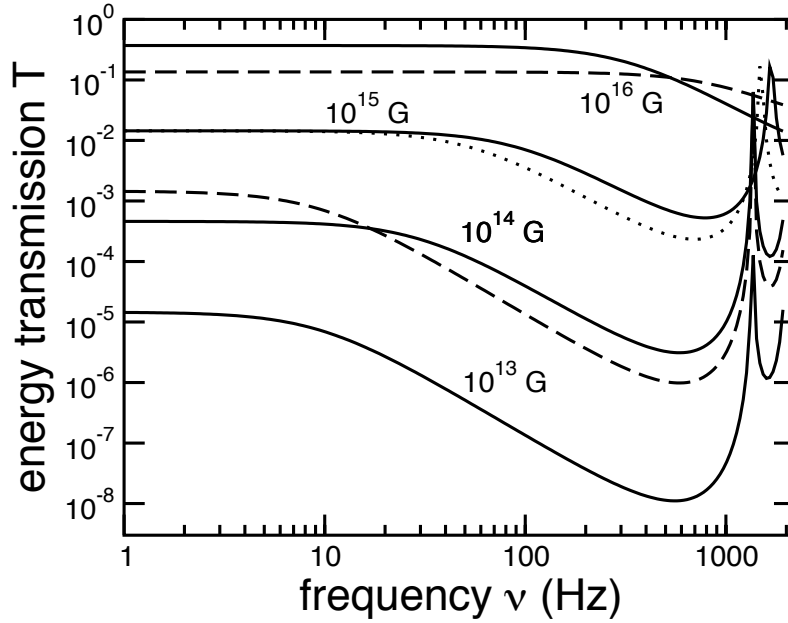


Figure 3. The transmission coefficient as a function of frequency. For frequencies above 10 – 100 Hz (depending on B), gradients in $\bar{\mu}$ and $\bar{\rho}$ increase the reflection of the wave back into the core, reducing T . Above ~ 1 kHz, transmission resonances appear in the simplified planar geometry. The solid curves show T for a core of superconducting protons, and the dashed curves are for normal protons; the curves are the same for $B = H_{c1} = 10^{15}$ G. The dotted curve for $B = 10^{15}$ shows the effect that perfect nuclear entrainment in the inner crust would have, corresponding to $\rho_d = \rho$. The core neutrons are assumed to be superfluid.

The dotted line shows the effect of perfect entrainment by nuclear clusters in the inner crust ($f = 1$). Entrainment increases the effective mass of nuclear clusters, reducing the shear speed for zero field, and reducing T . Because a fraction of the neutron superfluid does not move with the nuclei, the shear speed is increased, and T increases by a factor of ~ 3 at most.

The propagation of seismic energy from the crust into the magnetosphere was studied by Blaes et al. (1989) in the context of gamma-ray bursts from neutron stars assuming shallow energy deposition, at a density less than the neutron drip density. They found the existence of an evanescent wave zone very close to the stellar surface that is not found in the analysis given here. To evaluate the transmission coefficient, they evaluated $\tilde{\mu}ck_c$ in eq. [11] at the base of the evanescent wave zone. Eq. [11] applies only at low frequency, and only for the case that a wave zone exists for $z < 0$. Blaes et al. (1989) considered transmission for frequencies in the range $10^3 < \nu < 10^5$ Hz. Given the different boundary conditions and frequency regimes, a direct comparison to their work is not possible.

6 TRAPPING OF ENERGY IN THE CORE

Shear waves trapped in the core carry energy across the core at a speed equal to the wave group velocity, $c_s = c_{cv}$ for superconducting core protons, and $c_s = c_A$ for normal protons. The wave crossing time is $\simeq 2R/c_s$. The ‘attempt frequency’ is $c_s/2R$, with an energy transmission probability $T(\nu)$ per attempt, so the energy transmission rate is $\sim (c_s/2R)T(\nu)$ for a mode of frequency ν . The associated trapping time for energy in the core is thus

$$t_{\text{trap}} \simeq \frac{2R}{c_s T(\nu)}. \quad (21)$$

The trapping time is shown in Fig. 4. The spin-down rates for both SGR 1900 and SGR 1806 imply a dipole field of strength $B \simeq 10^{15}$ G. The trapping time is ~ 5 s below 100 Hz, and up to ~ 100 s at higher frequencies. These time-scales greatly exceed the observed rise time of $\lesssim 10$ ms that is seen in both giant flares and in small bursts. Even if $B = 10^{16}$ G, which is much larger than the field implied by the observed spin-down rates, energy cannot enter the magnetosphere from the core nearly quickly enough to explain observed rise times. Note that these trapping times represent lower limits, since the most favourable magnetic geometry for coupling of the stellar interior to the magnetosphere was assumed. These results strongly suggest that the flares are powered by the release of magnetic energy directly into the magnetosphere, not in the core.

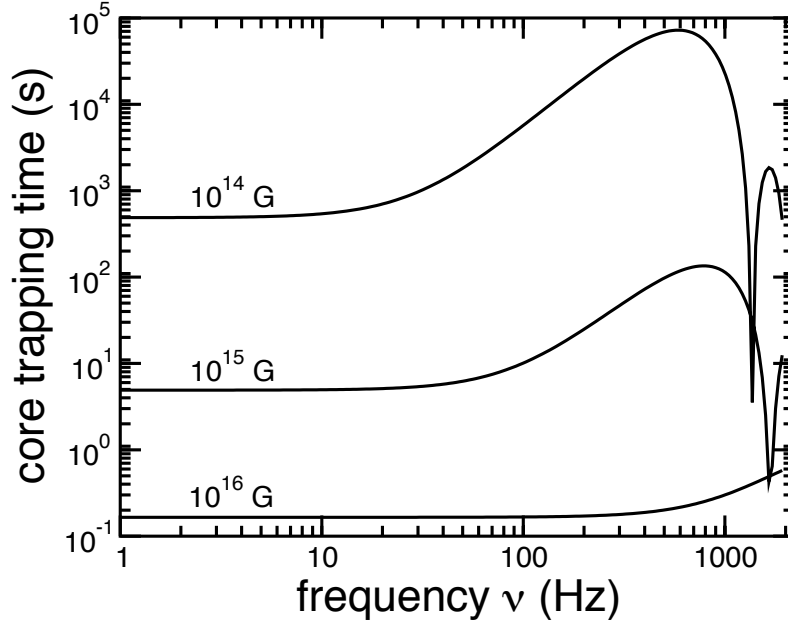


Figure 4. The trapping time for waves in the core. For $B = 10^{16}$ G, the core protons are assumed to be normal. These time-scales are lower limits (see the text).

7 EFFECTS OF REALISTIC FIELD GEOMETRIES

The analysis so far treats the magnetosphere as having infinite extent. Energy is transferred most efficiently to the magnetosphere when it excites field lines that are long enough to resonate with the wave that propagates from the core; coupling to shorter field lines will be greatly reduced, as will the transmission coefficient integrated over the stellar surface. For a field line of length L with two fixed foot-points on the star, the fundamental frequency is $c/2L$. Field lines with fundamental frequencies below 1 kHz are longer than 150 km. Most of the field lines that emerge from star are much shorter length than this, so the mechanical coupling between the stellar interior and the magnetosphere is poor. The energy flux into the magnetosphere will be reduced by a factor of $A/4\pi R^2$ with respect to the spherically symmetric situation, where A is the area of the star that is connected to field lines that are long enough to resonate with seismic waves. Though the transmission coefficient $T(\nu)$ has been calculated in a planar approximation for simplicity, a good final estimate for the transmission rate integrated over the stellar surface is $T(\nu)A/4\pi R^2$.

To estimate A , recall that the field line configuration from a magnetic dipole is given by

$$\frac{r}{R} = \left(\frac{\sin \theta}{\sin \theta_L} \right)^2, \quad (22)$$

where (r, θ) are spherical coordinates measure with respect to the magnetic dipole moment, and θ_L is the angle the field line takes at $r = R$ (the stellar surface in this simple approximation). Integration of eq. [22] along any given line gives the length of the field line L in the limit $\theta_L \ll 1$:

$$L \simeq 3.6R \sin^{-2} \theta_L. \quad (23)$$

If the power spectrum of excited magnetospheric waves ends at a cut-off ν_c , corresponding to a value $\theta_{L,\max}$ from eq. [23], the area of the magnetic polar region through which Alfvén waves enter the star is approximately $A \simeq \pi(R\theta_{L,\max})^2 \simeq 10^{-4}4\pi R^2 \nu_c(\text{Hz})$. Taking $\nu_c = 1$ kHz, indicates that the energy transfer into the magnetosphere could be reduced by a factor of about 10, raising the curves in Fig. 4 by the same factor. If ν is closer to 100 Hz, as suggested by the estimates of §2.2 assuming global readjustment of interior magnetic field, the curves of Fig. 4 go up by a factor of about 10^2 . The trapping time for $B = 10^{15}$ G becomes ~ 400 s to ~ 3 h for $\nu < 1$ kHz.

8 TRAPPING OF ENERGY IN THE MAGNETOSPHERE AND QPO EXCITATION

That the trapping time for seismic energy in the star is much longer than observed rise times suggests that flares are driven by the release of energy stored in the magnetosphere, where magnetic energy might be converted to Alfvén waves and radiation much more quickly. If QPOs represent stellar oscillations, they might be excited by the absorption of the star of relativistic Alfvén waves from the magnetosphere. I now estimate this time-scale.

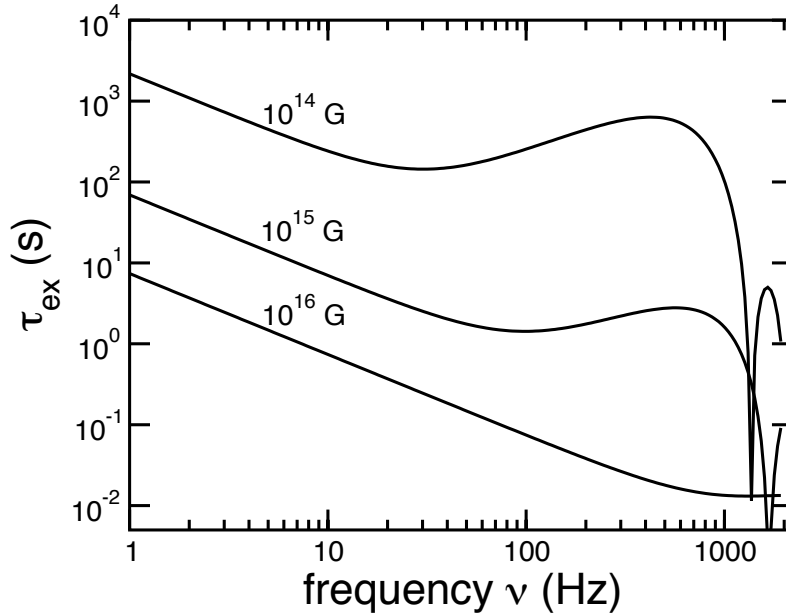


Figure 5. The time-scale over which Alfvén waves in the magnetosphere can excite stellar modes. The core protons are assumed to be normal for $B = 10^{16}$ G.

By energy conservation, the transmission coefficient for the excitation process is the same $T(\nu)$ calculated above. Since $T(\nu)$ is much less than unity for $1 \text{ Hz} < \nu < 1 \text{ kHz}$, the stellar surface is highly reflective to Alfvén waves. As a result, energy deposited in the magnetosphere will be trapped on closed field lines before it is either absorbed by the star or dissipated in the magnetosphere. A mode of frequency ν supported by closed field lines in the magnetosphere will bounce off the stellar surface at a rate ν , with an absorption probability $T(\nu)$ at each bounce. Ignoring dissipation in the magnetosphere, the absorption rate by the star of a magnetospheric Alfvén wave of frequency ν is $\nu T(\nu)$ for a planar geometry. As the energy is absorbed, it excites primarily shear waves in the crust and core (see §3). The characteristic excitation time-scale for a stellar mode of frequency ν by an Alfvén wave in the magnetosphere of frequency ν is

$$\tau_{ex} \sim [\nu T(\nu)]^{-1} \quad (24)$$

This time-scale is shown in Fig. 5. We see that for $B \geq 10^{15}$ G, most of the energy deposited in the magnetosphere could be absorbed by the star before the end of a giant flare, and so there could be sufficient time for relativistic Alfvén waves in the magnetosphere to excite stellar modes and associated QPOs. The strongest QPO seen in the tail of the giant flare in SGR 1806, at 92.5 Hz, was estimated to appear about two minutes into the flare (Israel et al. 2005; Strohmayer & Watts 2006).

Eq. [24] is a crude estimate. The field geometry near the surface of the star and inside the star is likely to be quite complicated, and certainly not everywhere perpendicular to the surface as assumed in this simple planar treatment. If the magnetospheric structure constrains the delivery of Alfvén energy to only small patches on the stellar surface, the energy transfer rate into the star could be greatly reduced, making τ_{ex} much longer. If this is the case, the interpretation of QPOs as magneto-stellar oscillations could be problematic. Calculations with more realistic field geometries are needed to resolve this issue; τ_{ex} calculated here is most likely a lower limit.

Suppose, however, that the magnetosphere changes its structure instantaneously. Now there is no time-scale in the problem, and all frequencies will be excited in the magnetosphere; f modes and torsional modes could be excited to large amplitudes (Levin & van Hoven 2011). More realistically, the time-scale for adjustment of the inner magnetosphere through an instability is $\sim R/c \simeq 30 \mu\text{s}$, implying a cut-off frequency of $\sim 30 \text{ kHz}$. The transmission coefficient generally increases with frequency, and high frequency waves could enter the star relatively easily.

A big uncertainty is the damping rate of Alfvén waves in the magnetosphere. In a magnetized plasma with a gradient in the Alfvén velocity, the case in the neutron star magnetosphere, dephasing of Alfvén waves drives currents and the wave can be quickly damped by electrical resistivity (Heyvaerts & Priest 1983). If the damping rate is too fast, the magnetosphere cannot excite global magneto-elastic modes. This problem merits further study.

9 CONCLUSIONS

The main conclusion of this paper is that the large impedance mismatch between the neutron star interior and the magnetosphere causes energy exchange between the two to be relatively slow. If the energy that drives a flare, either a small flare or a giant flare, is driven by *sudden*, global relaxation of the internal magnetic field, the trapped seismic energy takes at least seconds to minutes to reach the magnetosphere for $B = 10^{15}$ G (see Fig. 4), and possibly as long as minutes to hours for a realistic magnetic field geometry, in any case much longer than the observed rise times of < 10 ms. This conclusion rules out models of flares powered by *sudden*, internal magnetic relaxation (*e.g.*, Thompson & Duncan 1995, 2001). Crust failure cannot remove the fundamental impedance mismatch that limits the transfer of shear-wave energy from the core into the magnetosphere. *The energy that drives a flare must be stored in the magnetosphere.* One way this could happen is if the internal field gradually untwists, slowly twisting the magnetosphere until it becomes unstable (Lyutikov 2003). A lower limit to the rise time will be determined by the time-scale over which the instability develops. This time-scale could be $\lesssim 10$ ms for the tearing mode (Lyutikov 2006; Komissarov et al. 2007). The rise time of the observed flux could be longer, depending on the emission processes that accompany the instability.

The lower limits on the excitation time-scales of stellar modes by relativistic Alfvén waves in the magnetosphere given in Fig. 5 indicate that magneto-elastic oscillations of the star could be excited before the flare ends. Sudden readjustment of the magnetospheric configuration could excite frequencies up to ~ 30 kHz, which could deliver energy to the stellar interior relatively efficiently, though these frequencies are far higher than those of the observed QPOs. An important question is if Alfvén waves have time to excite global magneto-elastic modes before the Alfvén waves damp. I stress that it is not yet known if stellar oscillations can produce observable QPOs in the emission, though the mechanism of Timokhin et al. (2008) appears promising.

Realistic microphysical inputs have been used in these analyses, but the conclusions have been drawn using models with simplified geometries. More realistic energy deposition physics and magnetic field geometries should be considered.

ACKNOWLEDGMENTS

I thank C. D’Angelo, C. Gundlach, Y. Levin, M. Lyutikov, C. Pethick, and A. Watts for enlightening discussions. I am grateful to A. Watts and Y. Levin for comments on the manuscript. This work was supported by NASA Award NNX12AF88G, NWO Visitor Grant 040.11.403 (PI A. Watts), a Monash Research Enhancement Grant (PI Y. Levin), and a Kevin Westfold Scholarship. I thank the Astronomical Institute Anton Pannekoek, University of Amsterdam, and Monash University, for their hospitality.

REFERENCES

- Akmal A., Pandharipande V., Ravenhall D., 1998, *Physical Review C*, 58, 1804
 Barat C., Chambon G., Hurley K., Niel M., Vedrenne G., Estulin I., Kurt V., Zenchenko V., 1979, *Astronomy and Astrophysics*, 79, L24
 Blaes O., Blandford R., Goldreich P., Madau P., 1989, *The Astrophysical Journal*, 343, 839
 Braithwaite J., 2009, *Mon. Not. Roy. Astron. Soc.*, 397, 763
 Brown E., Cumming A., 2009, *Astrophys. J.*, 698, 1020
 Cerdá-Durán P., Stergioulas N., Font J. A., 2009, *Mon. Not. Roy. Astron. Soc.*, 397, 1607
 Chamel N., 2005, *Nucl. Phys. A*, 747, 109
 Chamel N., 2012, *Phys. Rev. C*, 85, 035801
 Chamel N., 2013, *Physical Review Letters*, 110, 011101
 Chamel N., Haensel P., 2006, *Phys. Rev. C*, 73, 045802
 Cline T., Desai U., Pizzichini G., Teegarden B., Evans W., Klebesadel R., Laros J., Hurley K., Niel M., Vedrenne G., 1980, *The Astrophysical Journal*, 237, L1
 Colaiuda A., Beyer H., Kokkotas K. D., 2009, *Mon. Not. Roy. Astron. Soc.*, 396, 1441
 Colaiuda A., Kokkotas K. D., 2011, *Mon. Not. Roy. Astron. Soc.*, 414, 3014
 D’Angelo C., Watts A., 2012, *The Astrophysical Journal Letters*, 751, L41
 Douchin F., Haensel P., 2001, *Astron. Astrophys.*, 380, 151
 Duncan R. C., 1998, *Astrophysics J.*, 489, L45
 Easson I., Pethick C., 1977, *Physical Review D*, 16, 275
 Evans W., Klebesadel R., Laros J., Cline T., Desai U., Teegarden B., Pizzichini G., Hurley K., Niel M., Vedrenne G., 1980, *The Astrophysical Journal*, 237, L7

- Feroci M., Frontera F., Costa E., Amati L., Tavani M., Rapisarda M., Orlandini M., 1999, *The Astrophysical Journal Letters*, 515, L9
- Flowers E., Ruderman M., 1977, *The Astrophysical Journal*, 215, 302
- Gabler M., Cerdá-Durán P., Font J. A., Müller E., Stergioulas N., 2013, *Monthly Notices of the Royal Astronomical Society*, 430, 1811
- Gabler M., Cerdá-Durán P., Stergioulas N., Font J. A., Müller E., 2012, *Monthly Notices of the Royal Astronomical Society*, 421, 2054
- Gabler M., Cerdá-Durán P., Font J. A., Müller E., Stergioulas N., 2011, *Mon. Not. Roy. Astron. Soc.*, 410, L37
- Gavriil F. P., Kaspi V. M., Woods P. M., 2004, *The Astrophysical Journal*, 607, 959
- Gill R., Heyl J. S., 2010, *Monthly Notices of the Royal Astronomical Society*, 407, 1926
- Glampedakis K., Samuelsson L., Andersson N., 2006, *Mon. Not. Roy. Astron. Soc.*, 371, L74
- Haensel P., Pichon B., 1994, *Astron. Astrophys.*, 283, 313
- Haensel P., Potekhin A. Y., 2004, *Astron. Astrophys.*, 428, 191
- Hambaryan V., Neuhäuser R., Kokkotas K. D., 2011, *Astron. Astrophys.*, 528, 45
- Heyvaerts J., Priest E., 1983, *Astronomy and Astrophysics*, 117, 220
- Hurley K., Boggs S., Smith D., Duncan R., Lin R., Zoglauer A., Krucker S., Hurford G., Hudson H., Wigger C., et al., 2005, *Nature*, 434, 1098
- Hurley K., Cline T., Mazets E., Barthelmy S., Butterworth P., Marshall F., Palmer D., Aptekar R., Golenetskii S., Il'Inskii V., et al., 1999, *Nature*, 397, 41
- Israel G., Belloni T., Stella L., Rephaeli Y., Gruber D., Casella P., Dall'Osso S., Rea N., Persic M., Rothschild R., 2005, *The Astrophysical Journal Letters*, 628, L53
- Kaspi V. M., 2007, *Astrophysics and Space Science*, 308, 1
- Komissarov S., Barkov M., Lyutikov M., 2007, *Monthly Notices of the Royal Astronomical Society*, 374, 415
- Lee U., 2007, *Mon. Not. Roy. Astron. Soc.*, 374, 1015
- Levin Y., 2006, *Mon. Not. Roy. Astron. Soc.*, 368, L35
- Levin Y., 2007, *Mon. Not. Roy. Astron. Soc.*, 377, 159
- Levin Y., van Hoven M., 2011, *Monthly Notices of the Royal Astronomical Society*, 418, 659
- Link B., 2012, *Mon. Not. Roy. Astron. Soc.*, 421, 2682
- Lyutikov M., 2003, *Mon. Not. Roy. Astron. Soc.*, 346, 540
- Lyutikov M., 2006, *Monthly Notices of the Royal Astronomical Society*, 367, 1594
- Mazets E., Golenetskii S., 1981, *Astrophysics and Space Science*, 75, 47
- Mazets E., Golenetskii S., Il'Inskii V., Aptekar R., Guryan Y. A., 1979, *Nature*, 282, 587
- Mendell G., 2002, *Mon. Not. Roy. Astron. Soc.*, 296, 903
- Mereghetti S., 2008, *The Astronomy and Astrophysics Review*, 15, 225
- Mereghetti S., Esposito P., Tiengo A., Zane S., Turolla R., Stella L., Israel G., Götz D., Feroci M., 2006, *The Astrophysical Journal*, 653, 1423
- Nakagawa Y. E., Mihara T., Yoshida A., Yamaoka K., Sugita S., Murakami T., Yonetoku D., Suzuki M., Nakajima M., Tashiro M., et al., 2008, *PASJ*, 61, S387
- Palmer D. M. e. a., 2005, *Nature*, 434, 1107
- Passamonti A., Lander S., 2013a, *Monthly Notices of the Royal Astronomical Society*, 429, 767
- Passamonti A., Lander S. K., 2013b, *MNRAS*, 438, 156
- Pethick C. J., Chamel N., Reddy S., 2010, *Prog. Theor. Phys. Suppl.*, 186, 9
- Piro A. L., 2005, *Astrophys. J.*, 634, L153
- Rea N., Israel G., Esposito P., Pons J., Camero-Arranz A., Mignani R., Turolla R., Zane S., Burgay M., Possenti A., et al., 2012, *The Astrophysical Journal*, 754, 27
- Rea N., Israel G., Pons J., Turolla R., Viganò D., Zane S., Esposito P., Perna R., Papitto A., Terreran G., et al., 2013, *The Astrophysical Journal*, 770, 65
- Rea N., Viganò D., Israel G. L., Pons J. A., Torres D. F., 2013, *ApJ*, 781, L17
- Samuelsson L., Andersson N., 2006, *Mon. Not. Roy. Astron. Soc.*, 374, 256
- Scholz P., Ng C.-Y., Livingstone M., Kaspi V., Cumming A., Archibald R., 2012, *The Astrophysical Journal*, 761, 66
- Sotani H., Kokkotas K. D., Stergioulas N., 2007, *Mon. Not. Roy. Astron. Soc.*, 375, 261
- Sotani H., Kokkotas K. D., Stergioulas N., 2008, *Mon. Not. Roy. Astron. Soc.*, 385, L5
- Steiner A. W., Watts A. L., 2009, *Phys. Rev. Lett.*, 103, 181101
- Strohmayer T. E., van Horn H. M., Ogata S., Iyemori H., Ichimaru S., 1991, *Astrophys. J.*, 375, 679
- Strohmayer T. E., Watts A. L., 2005, *Astrophys. J.*, 632, L111
- Strohmayer T. E., Watts A. L., 2006, *The Astrophysical Journal*, 653, 593

- Terasawa T., Tanaka Y. T., Takei Y., Kawai N., Yoshida A., Nomoto K., Yoshikawa I., Saito Y., Kasaba Y., Takashima T., et al., 2005, *Nature*, 434, 1110
- Thompson C., Duncan R. C., 1995, *Mon. Not. Roy. Astron. Soc.*, 275
- Thompson C., Duncan R. C., 1996, *Astrophys. J.*, 473, 322
- Thompson C., Duncan R. C., 2001, *The Astrophysical Journal*, 561, 980
- Tiengo A., Esposito P., Mereghetti S., Israel G., Stella L., Turolla R., Zane S., Rea N., Götz D., Feroci M., 2009, *Mon. Not. Roy. Astron. Soc.*, 399, L74
- Timokhin A., Eichler D., Lyubarsky Y., 2008, *The Astrophysical Journal*, 680, 1398
- van Hoven M., Levin Y., 2011, *Mon. Not. Roy. Astron. Soc.*, 420, 1036
- van Hoven M., Levin Y., 2012, *Monthly Notices of the Royal Astronomical Society*, 420, 3035
- Watts A. L., Reddy S., 2007, *Mon. Not. Roy. Astron. Soc.*, 379, 63
- Watts A. L., Strohmayer T. E., 2006, *Astrophys. J.*, 637, L117
- Woods P. M., Thompson C., 2006, in Lewin W. H. G., van der Klis M., eds, *Compact stellar X-ray sources Vol. 39*. Cambridge Astrophysics Series, Cambridge, p. 547